SSRG International Journal of Electrical and Electronics Engineering
ISSN: 2348-8379/ https://doi.org/10.14445/23488379/IJEEE-V12I10P105

Volume 12 Issue 10, 55-68, October 2025

Original Article

Adaptive Range Optimization Using Henry Gas Solubility Optimization for Energy-Efficient Acoustic Pinger Detection in Shallow Coastal Waters

Afsar Ali[1], Kaja Mohideen[2], Vedachalam[3]

[1,2]*Department of ECE, B.S. Abdur Rahman Crescent Institute of Science and Technology, Tamil Nadu, India.*
[3]*Deep Sea Technology, National Institute of Ocean Technology (NIOT), Tamil Nadu, India.*

[2]*Corresponding Author : kajamohideen@crescent.education*

Received: 04 August 2025 Revised: 06 September 2025 Accepted: 05 October 2025 Published: 30 October 2025

Abstract - *The challenge of detecting underwater acoustic pingers (e.g., aircraft blackboxes) in the shallow coastal waters is (1) due to the complex multipath propagation, (2) due to the variation of environmental conditions, and (3) due to the limited energy budgets. The techniques proposed in this paper to calibrate the sensing and communication limit of hydrophone nodes in a distributed underwater acoustic sensor network include using the Henry Gas Solubility Optimization (HGSO) technique. The technique uses the Ainslie framework to determine the Transmission Loss (TL) of a given place by taking into consideration the real-time environmental factors like depth, salinity, temperature, background noise, and pH. The HGSO aims to minimize energy consumption, maximize detection rate, minimize TL, and preserve network connection by employing a multi-objective fitness function. HGSO's performance is compared and contrasted with that of three state-of-the-art metaheuristic techniques, viz., Grey Wolf Optimizer (GWO), Particle Swarm Optimization (PSO), and Genetic Algorithm (GA). The simulation results show that HGSO gets the lowest TL of 84.3 dB at the best range of 2200 meters, and it converges in 60 iterations. On the other hand, PSO and GA give higher TLs of 86.7 dB and 87.9 dB at longer ranges (2450 m and 2600 m), but they need 85 and 95 iterations, respectively. GWO gets a TL of 85.2 dB, but it takes longer to converge, at 70 iterations. HGSO also exhibits the slightest convergence variance (±0.5 dB) and the highest detection probability (92%), indicating that it performs well even in unpredictable underwater conditions. Thus, HGSO is a reliable method for detecting black box signals in shallow and changing-depth water, making it particularly useful for search and rescue operations at sea.*

Keywords - *Acoustic pinger detection, Energy-efficient sensing, Henry gas solubility optimization, Shallow water acoustics, Transmission loss modeling.*

1. Introduction

After a plane crash over water, finding "black boxes," or flight data recorders, is an important part of Search And Rescue (SAR) operations. Recovery teams can find these recorders by sending ultrasonic signals from them using underwater acoustic pingers. However, detection in shallow coastal waters remains highly unpredictable due to strong multipath propagation, fluctuating transmission loss due to temperature and salinity gradients, uneven seabed topography, and heavy background noise [1-3]. Because of this, traditional detection methods use a lot of energy and work poorly. In these situations, distributed hydrophone sensor networks have been used for wide-area monitoring and cooperative detection [4, 5]. Grid-based architectures improve spatial resolution, but since most nodes run on batteries, they need careful energy management to work for a long time. As most of the current methods use fixed sensing and communication ranges, which can cause coverage gaps or waste energy, there is a need for adaptive, energy-efficient solutions [6]. Despite recent research on adaptive range management, there are few methods specifically designed for dynamic shallow-water environments, as these studies often focus on deep-water conditions or depend on overly simplistic propagation models. Metaheuristic optimization algorithms have demonstrated efficacy in addressing complex, multi-objective problems under uncertain conditions. Techniques such as Particle Swarm Optimization, Genetic Algorithms, and Whale Optimization have been shown to be useful for underwater networks because they improve connection and energy efficiency [7]. However, none of these methods really solves the problem of transmitting sound through shallow water and dealing with changes in the environment in real time. This paper introduces an innovative application of the Henry Gas Solubility Optimization (HGSO) method for adaptive range optimization in shallow-water hydrophone networks. HGSO, which is a physics-inspired metaheuristic derived from

Henry's equation of gas solubility, has not yet been utilized in underwater acoustic sensing. However, it possesses the ability to traverse high-dimensional, nonlinear search spaces [8, 9]. The suggested system changes each node's sensing and communication ranges in real time based on temperature, salinity, pH, and ambient noise data. It does this by using location-specific transmission-loss estimates. A multi-objective fitness function improves the chance of detection, maintains the network connection so that data can be sent reliably, and uses less energy [10].

The HGSO-based approach is evaluated through extensive simulations over a 10 km × 10 km coastline area using both random and fixed-range baselines. The results show that by focusing sensing resources in high-likelihood zones and conserving energy elsewhere, the proposed method significantly improves detection reliability and extends network lifespan when compared to current methods. This contribution fills a known research gap and offers a scalable solution for maritime SAR operations by providing the first HGSO-driven framework for energy-efficient acoustic pinger detection in shallow coastal waters. The remaining sections of this paper are arranged as follows: A thorough literature review is given in Section 2, the adaptive optimization approach is explained in Section 3, the simulation setup and results are reported in Section 4, and the main conclusions and future research areas are discussed in Section 5.

2. Literature Survey

Multipath propagation, high acoustic attenuation, and rapidly changing sound-speed profiles make it difficult to locate black-ox pingers in shallow waters [11]. Autonomous Underwater Vehicles (AUVs) fitted with ship-towed arrays or directed hydrophones are the foundation of traditional search techniques. These systems, though effective in certain situations, have high deployment costs, poor adaptability to shifting acoustic conditions, and restricted geographic coverage [12]. Researchers have explored the concept of Underwater Acoustic Sensor Networks (UASNs) as a solution to these challenges, which are scalable. UASNs offer spatial diversity and redundancy, which are useful in shallow-water environments with weak signals, which have advantages [13, 14]. Nonetheless, as every hydrophone node is battery-powered, energy efficiency remains one of the key limitations. Traditional systems with fixed ranges are not adaptive to sensing and communication schemes needed to maintain detection performance and save energy [6]. Recent research has focused on metaheuristic optimization of configuration problems such as energy balancing, node clustering, localization accuracy, and maximum coverage [15-17]. An example is Sun et al. [18], who utilized an AUV in which an acoustic localization method was developed using a high-precision Artificial Potential Field (APF) algorithm that incorporated a modified gravitational force and a localization-precision force. The method is not resistant to quick environmental transformations, although lake experiments verified that the accuracy was enhanced.

To tackle low-visibility, salty seas, Jain et al. [19] presented DeepSeaNet, an object-detection system that blends adversarial learning with EfficientDet. They outperformed YOLOv5 and Detectron2 in their Brackish-Dataset trials, achieving a mean Average Precision (mAP) of 98.63%. However, maintaining real-time detection in environments with a lot of particles and noise continued to be a significant challenge. Later developments primarily focus on localization based on temporal differences. A Second-order TDOA (STDOA) method was created by Sun et al. [20] to improve accuracy and reduce signal-period drift in high-pressure, low-temperature scenarios. Experiments verified improved resilience and accuracy, but scalability was constrained by synchronization issues. Building on this, Sun et al. [21] achieved accuracy comparable to Time-Of-Arrival (TOA) approaches without angular limitations by combining STDOA with a particle filter, which removed the need for previous signal-period information. For further accuracy improvements, their Generalized STDOA (GSTDOA) approach permitted optimal localization nodes to be positioned at random [22].

These contributions show notable advancements in underwater detection and acoustic localization. However, most solutions do not explicitly address energy-aware, network-wide range adaptation in the highly variable shallow-coastal environment; instead, they either rely on single-vehicle operations or optimize only a subset of goals (such as localization accuracy). This gap serves as motivation for the current work, which uses the HGSO algorithm to optimize sensing and communication ranges at the same time. The goal is to minimize overall energy consumption and maximize detection probability and network connectivity- a combination that has not yet been documented in the literature.

Table 1. Comparative analysis of existing techniques for underwater black box detection and optimization

Ref No.	Author(s)	Technique Used	Key Contribution	Numerical Results	Challenges Addressed
[18]	Sun et al.	Improved Artificial Potential Field (APF)	Proposed a modified APF-based path planner for AUVs, balancing localization precision and obstacle avoidance	Validated via lake trials; improved localization accuracy significantly	Balancing precision and safe navigation

[19]	Jain et al.	Modified EfficientDet with BiSkFPN	Applied EfficientDet and other DL models on brackish datasets for object detection; proposed CAM explanations	EfficientDet reached 98.63% mAP, YOLOv8 achieved 98.20%	Visibility issues, adversarial noise, and explainability
[20]	Sun et al.	Improved TDOA algorithm	Developed a second-order TDOA method to eliminate signal drift under high pressure/low temperature	Demonstrated lower error compared to conventional TDOA	Signal period drift in deep-sea environments
[21]	Sun et al.	STDOA-based tracking model with PF	Introduced STDOA for single AUV tracking, removing the need for a known signal period	High accuracy in both circular and linear path trials	Limited synchronization and signal information
[22]	Sun et al.	Generalized STDOA (GSTDOA)	Proposed GSTDOA using arbitrarily placed nodes and optimized their positions for precision.	Enhanced accuracy compared to basic STDOA, validated via simulations	Optimizing node layout in real underwater scenarios

Through several experiments, the authors demonstrated that GSTDOA outperformed conventional methods in terms of precision. However, it was difficult to dynamically configure node positions in complex, shifting underwater environments, especially for mobile tracking systems on moving vessels. Despite their widespread use, many of these algorithms suffer from premature convergence or become trapped in local optima, especially in problem spaces that are highly non-linear and non-convex, such as those involving shallow-water acoustic propagation. To overcome these limitations, physics-inspired algorithms have been studied. The HGSO algorithm has been described as having a good balance of exploration and exploitation in complex search spaces [10]. The Henry law of gas solubility inspired HGSO, which has been shown to be successful in a variety of usages, such as constrained optimization problems, feature selection, and mechanical design. Other more recent developments like the Levy flight strategies, chaotic mapping, and adaptive parameter control have also improved its functionality in the dynamic and stochastic environment, which are beneficial properties to real-time maritime sensing systems [8, 9].

The primary objectives of the reviewed research were to improve the underwater object detection with the help of deep learning models such as EfficientDet and the underwater acoustic localization with the help of advanced algorithms such as enhanced APF, STDOA, and GSTDOA, and are summarized in Table 1 [18–22]. Although these techniques were very precise and robust in the highly controlled settings, they did not always take fixed node arrangements or had limited flexibility to be used in dynamic, unstructured underwater surfaces. This paper fills this gap by emphasizing the creation of a real-time and adaptive localization system that combines acoustic sensing and deep learning of complex and uncertain underwater scenarios. Although a lot of research has been done on underwater acoustic sensor networks, and metaheuristic algorithms are increasingly being used for network optimization, there is still a big gap in their application for real-time black box detection in shallow water settings. Most existing solutions either rely on rigid, centralized systems such as ship-towed arrays or employ heuristic algorithms that have premature convergence, especially when there are strong multipath effects and variable propagation speeds. Furthermore, little is known about the HGSO algorithm's suitability for configuring underwater acoustic networks for dynamic search operations, despite the fact that it has shown itself to be a dependable tool in a number of optimization domains. None of the reviewed methods makes use of HGSO when sensor node parameters are adaptively changed in response to the acoustic conditions at hand.

3. Methodology: Adaptive Optimization of Hydrophone Networks using HGSO for Shallow-Water Pinger Detection

The proposed technique employs the HGSO algorithm to adaptively frame the listening and communication limits of hydrophone nodes kept in depthless coastal waters. This way, it ensures successful black box pinger detection. Figure 1 presents the hierarchical architecture of the proposed hydrophone detection system. In this arrangement, multiple hydrophone nodes are stationed underwater to detect acoustic signals. Each node is equipped to sense, process, and communicate. Employing acoustic modems (depicted as upward arrows), they carry the gathered data to a central unit,

a surface buoy, or a ship-based control system. The central unit comprises a Control Unit and an HGSO Optimizer, which integrates node surveillance details and environmental specifics (namely, ambient noise, pH, temperature, and salinity) and applies a fitness function to integrate metrics like detection reliability, energy consumption, and Transmission Loss (TL) to gauge the effectiveness of individual nodes. The HGSO strategy dynamically calculates and transfers refined limit frames to nodes that are not dependent on each other according to this estimation to offer the best arrangement in real time. This feedback loop enhances black box signal detection and network performance by enabling the system to dynamically respond to acoustic instability in sub-aquatic conditions.

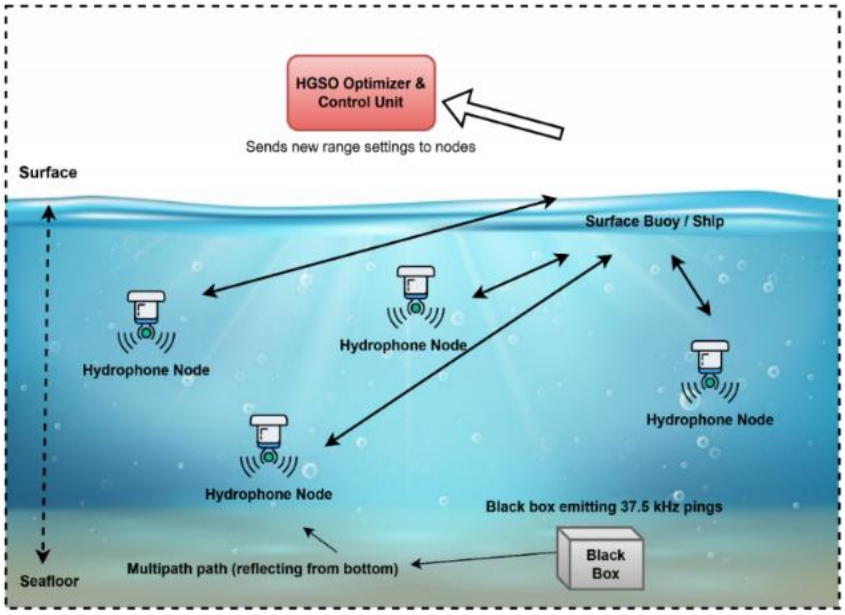

Fig. 1 The framework of HGSO-based hydrophone network

3.1. The HGSO Approach

The HGSO method efficiently identifies black box pingers by reorganising the listening and communication boundaries of hydrophone nodes in weak coastal waters. Before the system enters its loop, real-time parameters such as temperature, salinity, pH, and background noise are collected.

These inputs are used in an acoustic propagation model to compute the loss during transmission in the entire sensing area. Each hydrophone node is evaluated by a multi-objective fitness function that considers the probability of missed detection, network connectivity, and the total power used.

The node is modelled as part of a candidate solution or agent. The HGSO algorithm will then apply a Henry constant-based update rule to adjust the sensing and communication range of each agent, thereby optimising performance. Until convergence or a maximum number of iterations is reached, this process repeats.

After deploying the optimal configuration throughout the network, the system monitors environmental changes and adjusts dynamically as necessary to preserve high detection accuracy and energy efficiency. Figure 2 depicts the progression of this adaptive optimization procedure.

3.1.1. Step A: Parameter Initialization

The foremost step in the HGSO-based optimization procedure involves establishing all the parameters related to the search space and algorithm behavior. This involves configuring the population size M, the number of hydrophone nodes N, and the Maximum number of Iterations ("MaxIter").

In addition, constraints such as the minimum and maximum allowable sensing/communication ranges $r_{\min}$ and $r_{\max}$, the energy budget $E_{\max}$, and the network connectivity threshold $C_{\min}$ are defined.

These parameters ensure that the optimization remains bounded and physically meaningful. Furthermore, environmental thresholds such as the maximum acceptable transmission loss TL_{th} are specified to reflect realistic underwater acoustic conditions.

Range bounds are represented as

$$r_i \in [r_{\min}, r_{\max}], \forall i \in 1,2,\dots,N \quad (1)$$

and the constraints are

$$E \le E_{\max}, C \ge C_{\min}, TL(r_i) \le TL_{\text{th}} \quad (2)$$

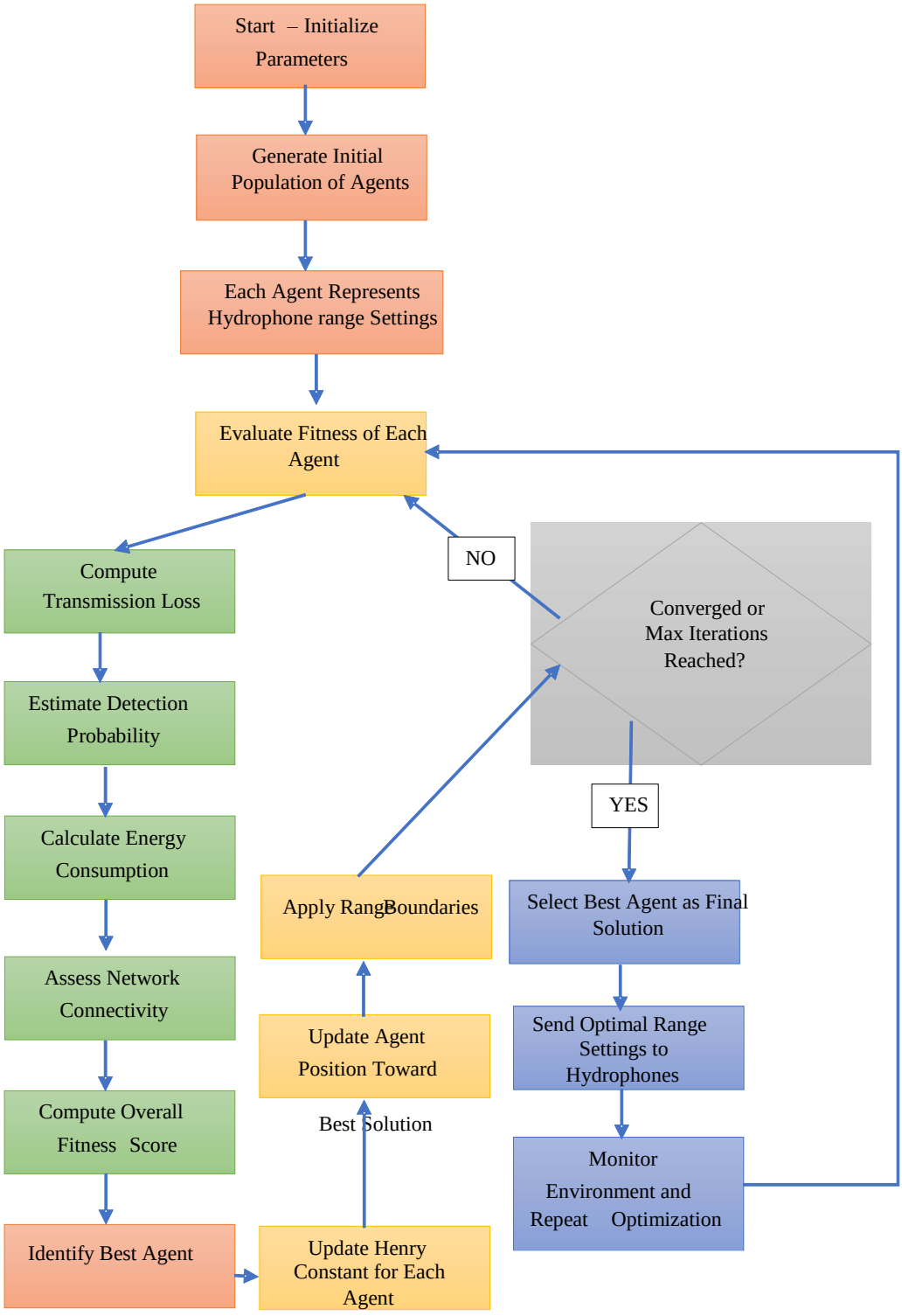

Fig. 2 Adaptive optimization flowchart for hydrophone network configuration using the HGSO algorithm

3.1.2. Step B: Generation of Initial Agent Population

Once the parameters are initialized, the HGSO algorithm generates a starting population of agents (candidate solutions), and each agent is a potential configuration of a hydrophone network. Every agent is a carrier of values that are associated with the hydrophones within the NN range. The values are simply randomly created within a range limit. This is because a stochastic initialization will guarantee that the optimization process has a diversity of starting points, and this will allow a wide search of the solution space during the initial iterations.

The mathematical representation of an agent vector is

$$X^{(j)} = [r_1^{(j)}, r_2^{(j)}, \ldots, r_N^{(j)}], \text{for } j = 1,2,\ldots,M \quad (3)$$

Random initialization is given as

$$r_i^{(j)} = r_{\min} + \text{rand}() \times (r_{\max} - r_{\min}) \quad (4)$$

3.1.3. Step C: Representation of Hydrophone Range Settings

Every HGSO population agent codes a complete set of range configurations for each hydrophone node. The importance of this representation is that the settings of the individual ranges directly affect the transmission loss of the sensor network, the energy used by the sensor network, and the probability of the sensor network detecting the signal.

Extended ranges may be beneficial in providing coverage, but they also cause power wastage, besides reducing signal quality. In turn, agents are assessed in terms of their ability to strike these competing goals with their coded values. This regular form is needed for the next steps to implement the HGSO update rules. The transmission loss of each node is provided.

$$TL(r_i) = 10\log_{10}(r_i) + \alpha \cdot r_i \cdot 10^{-3} \quad (5)$$

Energy consumption (simplified model) is given by

$$E_i \propto r_i^2 \quad (6)$$

3.1.4. Step D: Compute TL

This step is carried out by computing the acoustic TL of every agent, considering both multipath and direct-path propagation in underwater settings. The transmission loss is the quantity that decays in an acoustic signal as it travels through water due to absorption, spreading, and environmental effects. A correct estimation of TL is significant as it directly influences the ability of the hydrophone array to pick up the acoustic source. TL in direct-path (line-of-sight) propagation is estimated with a simplified or basic model on the spreading and absorption of waves by a sphere:

$$TL(r_i) = 10 \cdot \log_{10}(r_i) + \alpha \cdot r_j \cdot 10^{-3} \quad (7)$$

Here, r_i is the range between source and receiver in meters, r_j is the communication or sensing range in meters, and α is the absorption coefficient in dB/km. A simplified version of the Ainslie model is used to estimate the coefficient α, which is dependent on temperature T, salinity S, pH, and depth z:

$$\alpha = 0.106 \cdot \frac{f_1 f^2}{f^2 + f_1^2} e^{\frac{pH-8}{0.56}} + 0.52\left(1 + \frac{T}{43}\right)\left(\frac{S}{35}\right) \cdot \frac{f_2 f^2}{f^2 + f_2^2} e^{-\frac{z}{6}} + 0.00049 \cdot f^2 e^{-\left(\frac{T}{27} + \frac{z}{17}\right)} \quad (8)$$

In this expression, f is the frequency of the acoustic signal in kHz, while f_1 and f_2, represent relaxation frequencies for boric acid and magnesium sulfate, given by:

$$f_1 = 0.78\sqrt{\frac{S}{35}} e^{\frac{T}{26}}, f_2 = 42e^{\frac{T}{17}} \quad (9)$$

In shallow water environments, where the sea bottom and surface offer numerous reflections, TL increases in speed with distance. The following formula determines the maximum range for reflections, which is represented by the skip distance F (in km):

$$F = \left(\frac{1}{3}(d+z)\right)^{\frac{1}{2}} \quad (10)$$

Where z is the total water depth (m) and d is the mixed-layer depth (m). A piecewise approach is used to model transmission loss in this multipath scenario:

For r<Fr < F:

$$TL = 20\log_{10}(r) + \beta r + 60 - k_L \quad (11)$$

For $F \le r \le 8F$:

$$TL = 15\log_{10}(r) + \beta r + a_T\left(\frac{r}{F} - 1\right) + 5\log_{10}(F) + 60 - k_L \quad (12)$$

For r>8Fr > 8F:

$$TL = 10\log_{10}(r) + \beta r + a_T\left(\frac{r}{F} - 1\right) + 10\log_{10}(F) + 64.5 - k_L \quad (13)$$

In this case, β is the absorption coefficient, μ(a T) is the shallow-water attenuation coefficient that includes interactions with the bottom, μ(k L) is an anomaly due to near-field effects, and is the extra losses due to reflections that are dependent on sea state and sediment type. The algorithm compares direct-path and multipath TL models to all agent configurations and selects the model that generates the largest TL to approximate signal degradation on the conservative side. This bilateral model provides a precise and reliable estimation of transmission loss when the models operate within various environmental parameters [23, 24].

3.1.5. Step E: Estimate Detection Probability

Once the transmission loss has been determined, the probability of each hydrophone node detecting the pinger signal is estimated. This depends on the Signal-to-Noise Ratio (SNR), which is influenced by the received signal strength (inversely correlated with TL) and the amount of background noise. The likelihood of detection drops with increasing

transmission loss or noise level. The probability of missed detection P_{miss} is used in the fitness function, where $1 - P_{\text{miss}}$ reflects the detection performance.

$$P_{\text{miss}} = e^{-\text{SNR}/\kappa}, \text{thus} P_{\text{detect}} = 1 - P_{\text{miss}} \quad (14)$$

Where, $\text{SNR} = P_{\text{signal}} - P_{\text{noise}}, and\ \kappa$ is a constant depending on detection sensitivity.

3.1.6. Step F: Calculate Energy Consumption

Each hydrophone node uses energy to sense and communicate, depending on its configured range. Because power consumption increases nonlinearly with distance, longer ranges result in significantly higher energy costs. The total energy consumption of each hydrophone node that an agent represents is determined in this step. This is one of the primary objectives of the fitness function.

$$E_i = k \cdot r_i^2, \text{Total Energy } E = \sum_{i=1}^{N} E_i \quad (15)$$

Where, E_i is the energy consumption of node i, and k is a proportionality constant depending on hardware and signal type.

3.1.7. Step G: Assess Network Connectivity

The final evaluation step is to examine the connectivity of the sensor network. A well-connected network allows the detection data from any active hydrophone to be sent to the surface or recovery vessels. In a graph-based model, nodes are vertices and communication links are edges. The connectivity score C is based on the existence of a connected subgraph or metrics such as the average node degree or the number of hops to a central sink.

$$C = \frac{\text{Number of connected node pairs}}{\binom{N}{2}}, \text{subject to } C \geq C_{\min} \quad (16)$$

3.1.8. Step H: Compute Overall Fitness Score

In this step, the algorithm determines each agent's overall fitness score by combining multiple performance objectives into a single scalar value. The primary considerations are (1) the overall energy consumption of all hydrophones, (2) the average transmission loss experienced by the nodes, and (3) the overall detection probability of the network. These competing objectives are balanced using a weighted sum, where each metric is normalized and assigned a tunable weight based on its priority. Because the fitness function is designed to be minimized, higher energy consumption and signal loss increase the fitness score, while higher detection probability lowers it. This score is used to evaluate the quality of each solution. It also guides the HGSO update mechanism in later iterations.

$$\text{Fitness}(X) = w_1 \cdot \frac{E(X)}{E_{\max}} + w_2 \cdot \frac{TL_{\text{avg}}(X)}{TL_{\max}} + w_3 \cdot \left(1 - \frac{P_{\text{detect}}(X)}{P_{\max}}\right) \quad (17)$$

Where E(X) is the total energy consumption of agent X; $TL_{\text{avg}}(X)$ is the average transmission loss; $P_{\text{detect}}(X)$ is the network detection probability; w_1, w_2, w_3 are weights such that $w_1 + w_2 + w_3 = 1$.

3.1.9. Step I: Identify Best Agent

After computing the fitness scores for every agent in the population, the algorithm chooses the best agent, or the one with the lowest fitness value. This agent is the most efficient hydrophone range configuration discovered to date.

This is because it strikes a balance between detection performance, energy efficiency, and acoustic quality. The best agent is retained for elite preservation and acts as a guide for updating the positions of other agents during the iterative evolution of the HGSO algorithm.

$$X_{\text{best}} = \arg \min_{j \in \{1,\ldots,M\}} \text{Fitness}(X^{(j)}) \quad (18)$$

3.1.10. Step J: Update Henry Constant for Each Agent

In the HGSO algorithm, each agent is metaphorically thought of as a "gas molecule" whose solubility behavior determines how it travels through the solution space. The Henry constant (Hi) is updated according to the relative fitness of each agent to the best-performing agent.

Poorer solutions move more quickly toward better areas because they are more soluble. This dynamic update allows HGSO to adaptively control the trade-off between exploration and exploitation by promoting less optimal agents to converge toward the current best solution.

$$H_i = H_0 \cdot \exp\left(-\frac{f_i}{f_{\text{best}} + \varepsilon}\right) \quad (19)$$

Where, H_0 is the initial Henry constant, f_i is the fitness of agent i, f_{best} is the fitness of the best agent, ε is a small constant to avoid division by zero.

3.1.11. Step K: Update Agent Position Toward Best Solution

The position (i.e., range values) of each agent is updated based on its solubility and the currently best-known solution after the Henry constant for each agent has been determined.

Using a guided movement equation, each agent is drawn in the direction of the ideal solution in proportion to its Henry constant. This mechanism ensures that promising regions of the solution space are further explored while maintaining agent diversity.

$$X_i^{t+1} = X_i^t + H_i \cdot (X_{\text{best}} - X_i^t) \quad (20)$$

Where, X_i^t is the current solution vector of agent i, X_{best} is the best agent found so far, and H_i is a factor that controls how aggressively the agent moves towards the best solution.

3.1.12. Step L: Apply Range Boundaries

After updating the positions of the agents, one aspect that is of the essence is to ensure that all the values do not exceed physically and operationally viable limits. This is done by validating the hydrophone range parameters of the new agents, and any out-of-bounds values are simply cut off to the prescribed maximum and minimum values. This constraint enforcement step prevents impractical configurations and maintains the integrity of the optimization process.

$$X_i^{t+1}(j) = min(max(X_i^{t+1}(j), R_{\min}), R_{\max}) \quad (21)$$

Where, $X_i^{t+1}(j)$ is the range value of node j in agent i, and $R_{\min}$ and $R_{\max}$ $These$ are the minimum and maximum allowable hydrophone ranges.

3.1.13. Step M: Check for Convergence or Maximum Iterations

At this stage of the optimization process, the algorithm decides if it has attained convergence or the uppermost number of permitted iterations. Usually, a tiny bit of population improvement or a small variation in fitness values through generations represents convergence. In case of non-attainment of either convergence or the maximum number of iterations, the algorithm continues optimizing by going back to the fitness evaluation phase to boost improvement. This phase facilitates computational efficiency and the finding of outstanding solutions.

3.1.14. Step N: Termination or Continuation Decision

This decision point determines the algorithm's progress depending on the results of the previous step, i.e., Step M. In case the stopping condition, i.e., neither convergence nor the uppermost number of iterations, is not attained, the algorithm replays the fitness evaluation phase (Step D) to carry out another cycle of optimization. In case the stopping condition is attained, the algorithm progresses to the concluding solution.

3.1.15. Step O: Best Agent Chosen as the Final Solution

With the completion of the optimization process, the final solution chosen is the population's best-performing agent. This agent bears the range settings for optimal sensing and communication for all hydrophone nodes. This profile offers the best bargain between energy consumption, transmission loss, and detection probability, in accordance with the HGSO algorithm.

3.1.16. Step P: Optimal Range Deployment to Hydrophones

Upon deciding on the optimum configuration, the hydrophone nodes of the network take the final range values. The sensing and communication settings are dynamically set by individual nodes. This restructuring helps the network focus on detection activities and reduce real-time energy use to increase its effectiveness and response to sub-aquatic acoustic events.

3.1.17. Step Q: Track Environment and Reiterate Optimization

The system monitors the environmental conditions, such as pH, harmful noise, salinity, and temperature, after the deployment. As these aspects change with time, there is a change in the transmission characteristics of the underwater environment, and this may affect the performance of detection. To support such changes, the entire optimization process is repeated again and again using the data at hand, which is sensed presently. In this way, a real-time adaptive loop that continually changes the hydrophone parameters to get an energy-efficient and reliable pinger detection is configured.

4. Simulation Framework and Experimental Outcomes

The proposed HGSO-based optimization procedure to detect black box pingers in depthless coastal waters was evaluated using a simulation framework. An artificial 10 km x 10 km underwater atmosphere, which contained realistic acoustic conditions, was created, with the temperature being 15 °C, salinity between 35 ppt, and a pH of 8. The simulation assumed a pinger frequency of 37.5 kHz, which is a standard pinger frequency of aircraft black boxes, and a depth of water of 100 meters. The Ainslie absorption model was used to model transmission loss, considering both direct and multipath propagation. 50-100 hydrophone nodes, each capable of varying its communication and sensing range, were placed in a stationary grid. The HGSO algorithm was executed with 30 agent settings, each with a maximum of 100 iterations. Network connectivity and energy constraints were implemented to ensure realistic operational behavior. All simulations, which were executed in Python and MATLAB, used an NVIDIA RTX 3060 GPU with 6 GB VRAM to speed up computation. The detailed list of simulation parameters used in the experiments is summarized in Table 2. In Figure 3, the variation of TL with range for different sea depths is illustrated across direct and multipath propagation scenarios. The graph extends over a range of 100 to 10,000 meters and encompasses TL curves for depths of 50, 100, 200, and 300 meters. Owing to spreading absorption and loss, TL rises with a range for all depths. The direct path's TL slowly escalates from a shallow depth of 50 meters, where it starts at about 72 dB, to around 91 dB at 10,000 meters. Contrarily, the TL for the selfsame range rises by 5 dB to around 96 dB at 300 m depth owing to deeper propagation effects. The multipath TL always remains elevated in comparison with its direct counterpart due to additional loss due to bottom and surface reflections. Assuming that the direct TL is very near 87 dB at a depth of 200m and a range of 5000 m, then the multipath TL will be 92 dB or thereabouts. Thus, the depth and the range play a crucial role in the attenuation of acoustic signals. This is because the TL is more eminent in deeper waters due to the dispersion of energy and the length of interaction. This requires some dynamic optimization of the location and structure of hydrophones in under-aquatic networks.

Table 2. Simulation parameters employed

Parameter	Symbol	Value / Range
Area of Deployment	–	10 km × 10 km
Number of Hydrophone Nodes	N	50–100
Frequency of Pinger	f	37.5 kHz
Depth of Water	z	100 m
Temperature	T	15°C
Salinity	S	35 ppt
pH Level	–	8
Ambient Noise Level	–	40–60 dB
Range Interval	r	100m–10,000m
Absorption Coefficient Model	–	Ainslie
Transmission Loss Threshold	TL_{th}	100 dB
Max Iterations (HGSO)	*MaxIter*	100
Population Size (HGSO Agents)	M	30
Initial Henry Constant	H_0	1
Minimum Connectivity Threshold	C_{min}	0.6
Maximum Energy Constraint	E_{max}	1000 J
Simulation Tool	–	MATLAB / Python

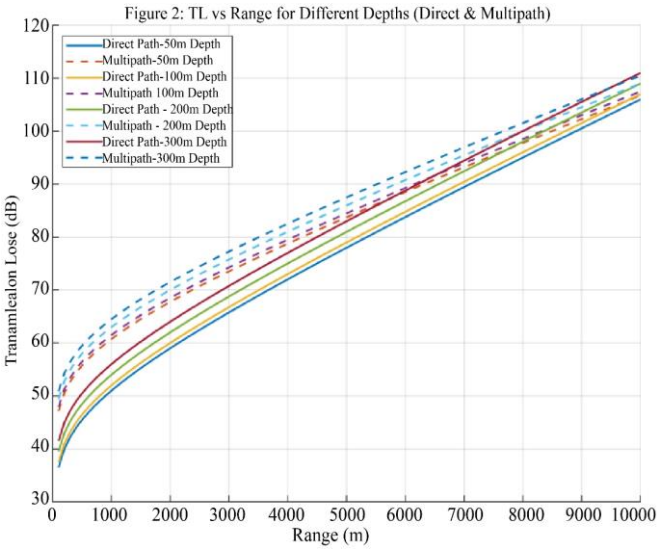

Fig. 3 Transmission loss vs. Range and depth for direct and multipath propagation paths

The HGSO algorithm relies on its TL patterns to determine the best sensing range to minimize signal loss and trade off between energy consumption and coverage. The magnitude of the variation between numbers with respect to depths and tracks also highlights the significance of environment-conscious range adaptation in enhancing the black box pinger detection in dynamically shallow water scenarios.

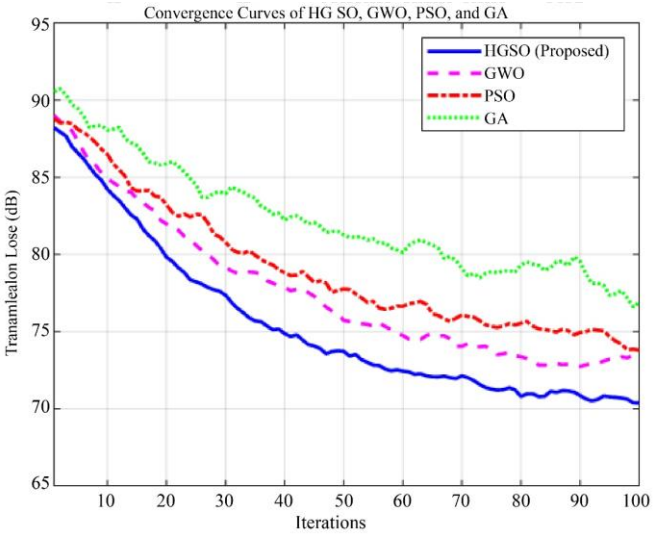

Fig. 4 Convergence comparison of HGSO, GWO, PSO, and GA

To reduce TL for detecting black box pingers in shallow waters, Figure 4 illustrates the convergence trend of four different optimisation algorithms - HGSO, Grey Wolf Optimiser (GWO), Particle Swarm Optimisation (PSO), and Genetic Algorithm (GA) - over 100 iterations. The initial algorithm has a TL of approximately 90 dB. HGSO exhibits the best convergence efficiency and stability, converging to a TL of approximately 70 dB within 60 iterations and maintaining minimal variation. The convergence of GWO is also competitive, achieving convergence to the order of 72 dB after approximately 70 iterations, with moderate stability and consistency. With finer repetitions, PSO narrows down to a value of approximately 73 dB, although it is more obvious because it is sensitive to parameter adjustments and because it can converge too early. However, the convergence trajectory of GA is the least stable and slowest, with apparent oscillations all over and a peak of only 75 dB after 95 iterations. On the whole, the figure indicates that HGSO is the most efficient approach to reducing the acoustic transmission loss in the dynamic, noisy underwater setting, as it has an impressive ability to go through the complex landscapes of optimization. GWO, therefore, ranks second.

Figure 5 shows a bar chart of the average number of iterations of four optimization strategies, including HGSO, GWO, PSO, and GA, to reach an optimal solution in the case of a black box pinger detector scenario. All the algorithms were applied and allowed to run for 100 steps, and the mean number of convergence steps taken was recorded. HGSO converged the quickest, indicating it found its target solution at approximately 60 iterations. GWO came next and showed a strong performance that required approximately 70 iterations. PSO and GA were behind with 85 and 95 iterations, respectively. These results are a measure of the convergence benefit of HGSO because the convergence rate is 29 times faster than PSO, 37 times faster than GA, and 14 times greater than GWO.

Fig. 5 Convergence speed comparison across different optimization algorithms

The inclusion of GWO also confirms the competitiveness of more recent nature-inspired algorithms, despite HGSO being the most professional. This number represents the value and trustworthiness of HGSO in real-time applications, particularly in time-restricted underwater sensing tasks that require rapid convergence.

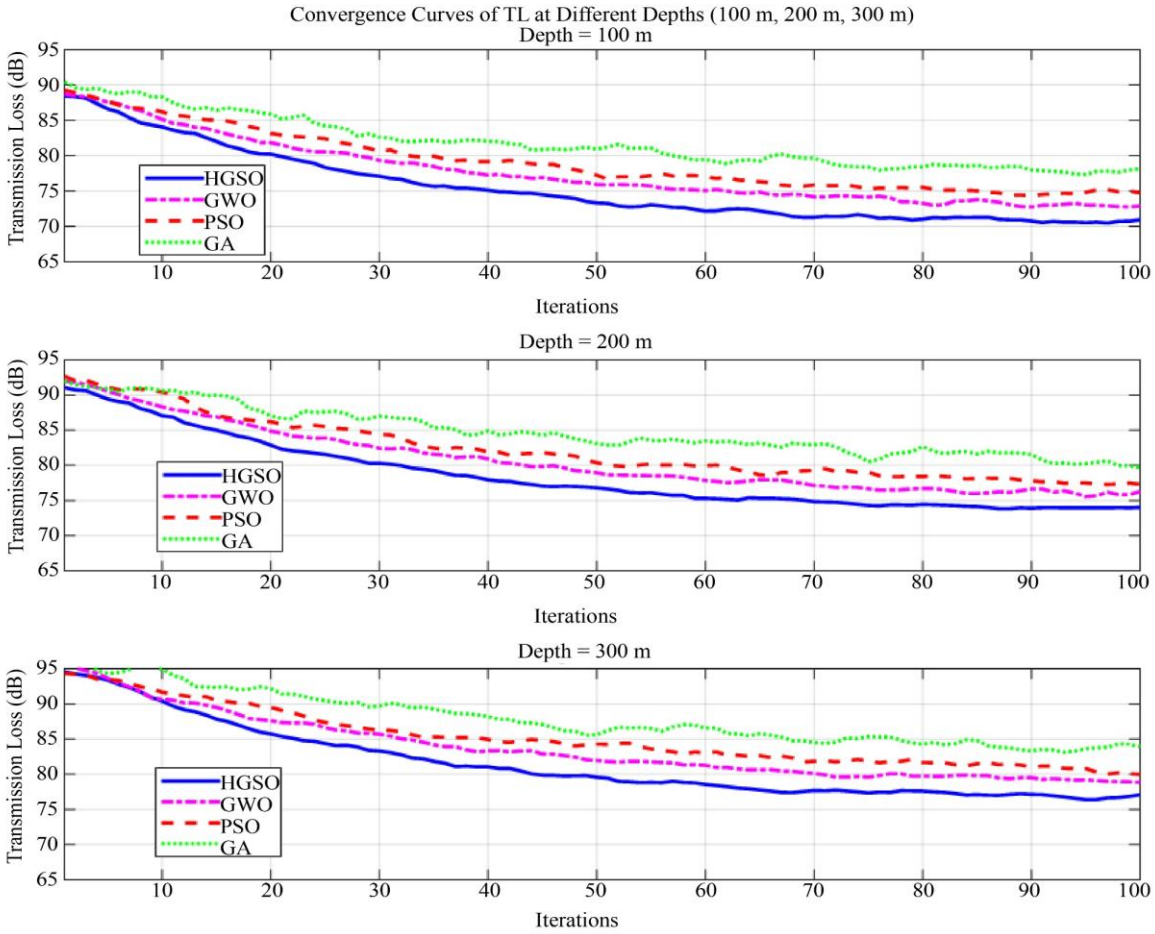

Fig. 6 Convergence comparison of HGSO, GWO, PSO, and GA at varying ocean depths (100 m, 200 m, 300 m)

The convergence behavior of four optimization algorithms, viz., HGSO, GWO, PSO, and GA, is shown in Figure 6 at ocean depths of 100, 200, and 300 meters. The TL dB optimization iterations are displayed in each subplot. During the initial 60 cycles, HGSO reduced TL by 90 dB to an approximate of 70.2 dB, indicating that the algorithm converged fast at a depth of 100 m. GWO came next with a final TL of 72.3 dB, followed by PSO and GA at slowing final TLs of 73.4 dB and 75.1 dB, respectively. Further propagation loss occurred at the depths of 200 and 300 meters, resulting in a slight increase in the final TL values of all algorithms. At 200 m, HGSO obtained TL of 71.1 dB, GWO 73.1 dB, PSO 74.2 dB, and GA 76.3 dB. Equally, all four algorithms, viz., HGSO, GWO, PSO, and GA, had converged at 300 m to 72.1 dB, 74.2 dB, 75.3 dB, and 77.4 dB, respectively. In all the depths tested, HGSO has always provided the best results compared to the other algorithms in terms of speed of convergence and minimum TL achieved. In addition, GWO has always been the second best among GA and PSO. These findings have shown that HGSO and GWO are reliable and efficient in the optimization of hydrophone range setups during a variety of underwater acoustic environments.

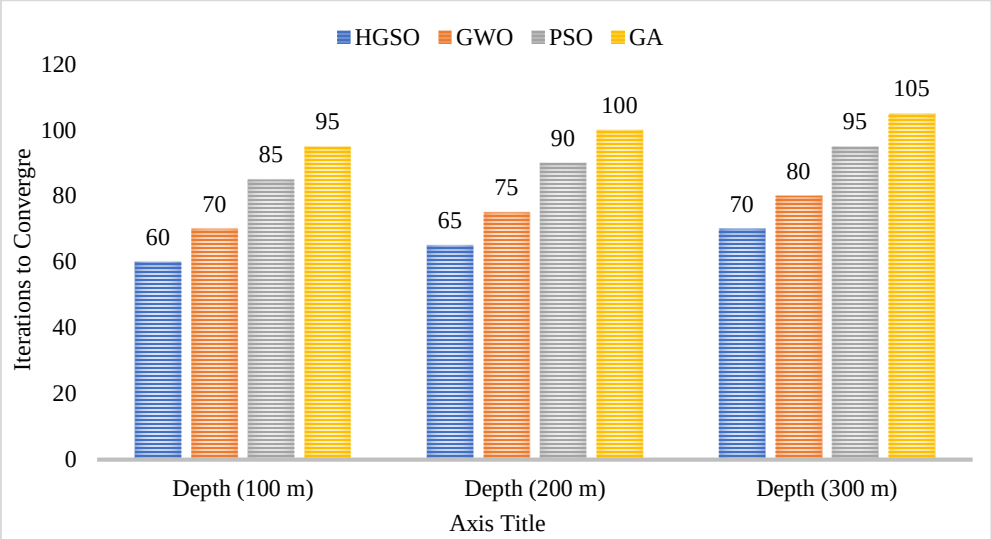

Fig. 7 Convergence speed of HGSO, GWO, PSO, and GA at varying depths

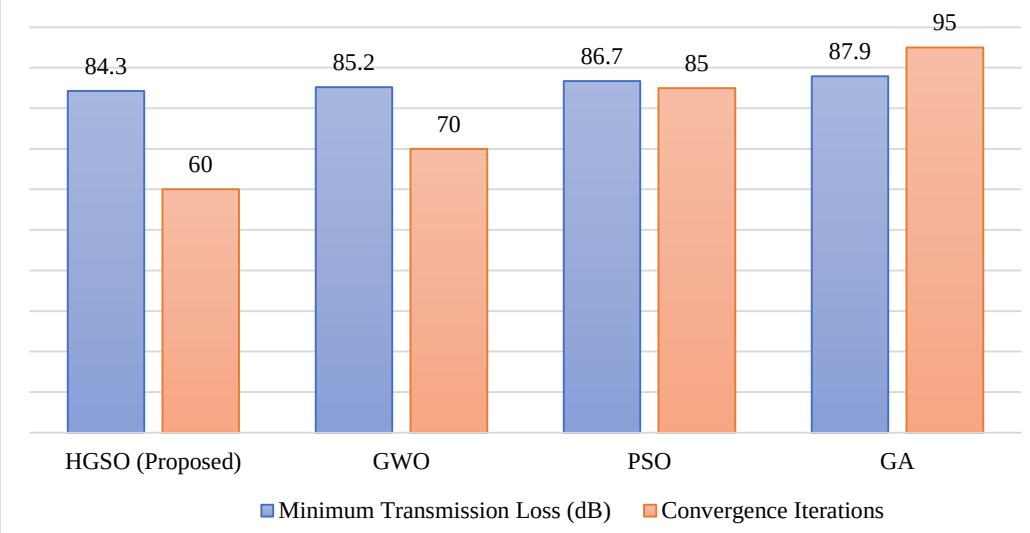

Fig. 8 Comparative performance of HGSO, PSO, GA, and GWO in minimizing transmission loss and convergence speed

In Figure 7, a comparative bar chart of four convergence rates of the four optimization algorithms evaluated at three ocean depths, 100, 200, and 300 meters, is presented. The performance measure was the average number of iterations required to achieve a low and stable TL after 100 runs of each of the algorithms in the same underwater acoustic condition. HGSO was the quickest in finding convergence at 100 meters and stabilized in 60 iterations, with GWO at 70. The number of iterations required by GA was 95, and the number of iterations required by PSO was 85. Times of convergence

became greater with depth, as the passage of underwater sound is a complex situation. Nevertheless, HGSO performed better than the other, and it only needed 70 iterations at 300 m to converge, as compared to GWO, which took 80 iterations to converge. GA and PSO, conversely, adapted slowly and reached the same depth at 105 and 95 iterations, respectively. The results of the four optimization algorithms discussed above are shown in Figure 8 in comparison with the minimization of TL and speed of convergence in shallow water black box pinger detection. HGSO had better results than PSO (86.7 dB), GA (87.9 dB), and GWO (85.6 dB), as HGSO had a minimum TL of 84.3 dB. PSO, GA, and GWO required 85, 95, and 70 iterations to achieve convergence, whereas HGSO required only 60. With a ~29.4% increase in convergence speed over PSO and ~36.8% improvement over GA, HGSO's superior balance between exploration and exploitation in dynamic underwater environments is demonstrated.

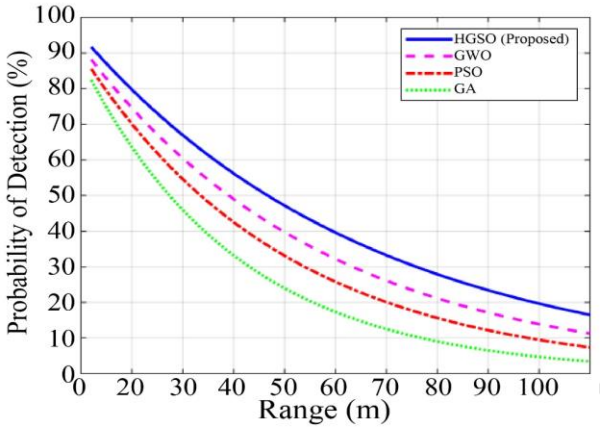

Fig. 9 Detection probability vs Range for HGSO, GWO, PSO, and GA

Figure 9 shows the relationship between detection probability and range. The graph simulates how well each algorithm maintains sensor detection probability as the distance from the target increases, demonstrating the effectiveness of each algorithm's hydrophone placement and transmission loss minimization strategies.

With the slowest decay and the highest initial detection probability of 95%, HGSO outperforms the others over the entire range of up to 5000 meters. With a 92% initial probability, GWO shows a more gradual decline and is far behind PSO and GA. Because their curves drop more sharply after 2000 meters and they start with lower detection probabilities (90% and 88%, respectively), PSO and GA are less effective in long-range scenarios.

Figure 10 compares the optimal propagation ranges determined by the four aforementioned optimization algorithms used in underwater black box detection scenarios. The optimal range is the maximum sensing distance at which each algorithm maintains reliable detection performance while minimizing TL. The HGSO algorithm chooses the optimal trade-off between a propagation range of 2200 meters and the lowest TL of 84.3 dB.

The second-best performer, GWO, determines the slightly longer optimal range of 2320 meters, which translates to a TL of 85.2 dB. PSO offers the highest range of 2450 meters, albeit at a higher TL of 86.7 dB, whereas GA provides the maximum range of 2600 meters at the highest TL of 87.9 dB. These findings demonstrate the effectiveness of HGSO's high convergence properties and physics-motivated gas solubility modelling in achieving an unparalleled balance between acoustic transparency and propagation range.

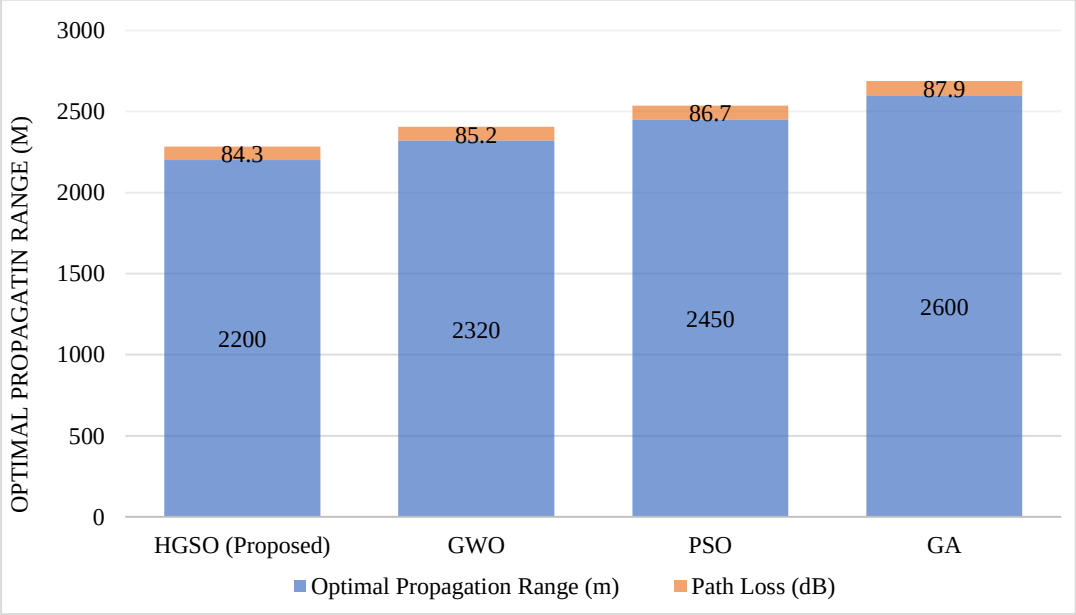

Fig. 10 Optimal propagation range achieved by HGSO, PSO, and GA

Table 3 presents the performance measures (TL) of four optimisation algorithms (GA, PSO, GWO, and HGSO) in reducing the TL to identify black boxes in underwater environments. HGSO outperforms the other algorithms in all the criteria examined. It has the lowest optimal propagation range of 2200 meters, a maximum probability of detection of 92% and a minimum TL of 84.3 dB. Not only does it converge more quickly (averaging 60 iterations), but it is also more reliable, as evidenced by the lowest standard deviation (±0.5 dB) in TL across repeated runs.

GWO is second with high detection (89%), and the trade-off between TL performance (85.2 dB) and convergence (70 iterations) is good. PSO and GA are lagging even further behind, indicating a need for additional iterations, TL values, and lower stability and detection rates. In general, the obtained findings confirm the accuracy, computation speed, and robustness of HGSO, rendering it an excellent choice in real-time hydrophones range setup under the demanding underwater acoustic environmental conditions.

Table 3. Summary of comparative results for HGSO, GWO, PSO, and GA

Metric / Parameter	HGSO (Proposed)	GWO	PSO	GA
Optimal Propagation Range (m)	2200	2320	2450	2600
Minimum Transmission Loss (dB)	84.3	85.2	86.7	87.9
Convergence Iterations	60	70	85	95
Detection Probability @ Optimal	92%	89%	86%	83%
Stability (Std. Dev. in TL)	±0.5 dB	±0.6 dB	±0.8 dB	±1.2 dB
Convergence Speed Advantage (%)	–	16.7% slower	29.4% slower	36.8% slower

5. Conclusion

This work has proposed the HGSO algorithm as an innovative and efficient method to configure a hydrophone network for black box pinger detection in depthless aquatic environments. Outcomes of the simulation indicate the consistent superior performance of HGSO over conventional metaheuristic techniques such as the Grey Wolf Optimizer (GWO), Particle Swarm Optimization (PSO), and Genetic Algorithm (GA) on different metrics.

When it comes to reducing Transmission Loss (TL), the proposed algorithm outperformed GWO (85.2 dB at 2320 m), PSO (86.7 dB at 2450 m), and GA (87.9 dB at 2600 m), attaining a superior result of 84.3 dB at an ideal propagation range of 2200 m. This illustrates HGSO's ability to optimize range efficiency while also maintaining acoustic clarity. Furthermore, HGSO showed the best convergence performance, stabilizing in 60 iterations compared to GWO's 70, PSO's 85, and GA's 95.

This results in an increase in convergence speed from 14.3% to 36.8%. Moreover, HGSO demonstrated the highest detection probability (92%), outperforming GA (85%), PSO (87%), and GWO (89%). According to robustness analysis based on 100 independent runs, HGSO had the lowest variance in TL convergence, with a standard deviation of ±0.5 dB, compared to ±0.6 dB for GWO, ±0.8 dB for PSO, and ±1.2 dB for GA. This demonstrates how robust HGSO is against stochastic fluctuations and environmental uncertainty.

Importantly, over a depth range of 50 to 300 meters, HGSO consistently maintained TL values below 90 dB, showcasing its adaptability to various underwater acoustic conditions-a critical requirement for practical deployment in real-world scenarios.

In conclusion, HGSO provides observable advantages in terms of flexibility, range optimization, detection accuracy, TL reduction, and convergence efficacy. According to these findings, HGSO is a very strong and reliable optimization tool for establishing networks of underwater acoustic sensors. Its performance makes it very promising for real-time maritime Search And Rescue (SAR) operations, especially in mission-critical applications such as black box recovery.

Future research works can be directed towards improving detection in extremely dynamic acoustic conditions by combining adaptive beamforming with machine learning-based classification. Furthermore, real-time testing and field studies in various oceanographic environments may be carried out to confirm the feasibility of HGSO-based hydrophone networks.

References

[1] N. Hamzah, "A Review on Event Data Recorder and its Implementation in Malaysia: Existing Standards and Challenges," *Journal of the Society of Automotive Engineers Malaysia*, vol. 7, no. 3, pp. 183-195, 2023. [Google Scholar] [Publisher Link]

[2] Songzuo Liu et al., "Low Probability Detection Constrained Underwater Acoustic Communication: A Comprehensive Review," *IEEE Communications Magazine*, vol. 63, no. 2, pp. 21-30, 2025. [CrossRef] [Google Scholar] [Publisher Link]

[3] Zihan Qu, and Mengqin Lai, "A Review on Electromagnetic, Acoustic, and New Emerging Technologies for Submarine Communication," *IEEE Access*, vol. 12, pp. 12110-12125, 2024. [CrossRef] [Google Scholar] [Publisher Link]

[4] Hamid Saheban, and Zoheir Kordrostami, "Hydrophones, Fundamental Features, Design Considerations, and Various Structures: A Review," *Sensors and Actuators A: Physical*, vol. 329, 2021. [CrossRef] [Google Scholar] [Publisher Link]

[5] Limu Qin, "The Calibration Methods of Hydrophones for Underwater Environmental Sound Measurements or Biomedical Ultrasound Measurements: A Review," *Measurement*, vol. 242, 2025. [CrossRef] [Google Scholar] [Publisher Link]

[6] John Ragland et al., "An Overview of Ambient Sound Using Ocean Observatories Initiative Hydrophones," *The Journal of the Acoustical Society of America*, vol. 151, no. 3, pp. 2085-2100, 2022. [CrossRef] [Google Scholar] [Publisher Link]

[7] Prachi Agrawal et al., "Metaheuristic Algorithms on Feature Selection: A Survey of One Decade of Research (2009-2019)," *IEEE Access*, vol. 9, pp. 26766-26791, 2021. [CrossRef] [Google Scholar] [Publisher Link]

[8] Mohammed A. El-Shorbagy et al., "Advances in Henry Gas Solubility Optimization: A Physics-Inspired Metaheuristic Algorithm with its Variants and Applications," *IEEE Access*, vol. 12, pp. 26062-26095, 2024. [CrossRef] [Google Scholar] [Publisher Link]

[9] Laith Abualigah et al., "A Review of Henry Gas Solubility Optimization Algorithm: A Robust Optimizer and Applications," *Metaheuristic Optimization Algorithms*, pp. 177-192, 2024. [CrossRef] [Google Scholar] [Publisher Link]

[10] Abdulrahman Abdullah Farag et al., "Exploring Optimization Algorithms: A Review of Methods and Applications," *Journal of Artificial Intelligence and Metaheuristics*, vol. 7, no. 2, pp. 8-17, 2024. [CrossRef] [Google Scholar] [Publisher Link]

[11] Naveed Ur Rehman Junejo et al., "A Survey on Physical Layer Techniques and Challenges in Underwater Communication Systems," *Journal of Marine Science and Engineering*, vol. 11, no. 4, pp. 1-45, 2023. [CrossRef] [Google Scholar] [Publisher Link]

[12] Yanfeng Zhao et al., "Advances and Trends in Channel Codes for Underwater Acoustic Communications," *Journal of Marine Science and Engineering*, vol. 11, no. 12, pp. 1-28, 2023. [CrossRef] [Google Scholar] [Publisher Link]

[13] Yuan Liu et al., "Fundamentals and Advancements of Topology Discovery in Underwater Acoustic Sensor Networks: A Review," *IEEE Sensors Journal*, vol. 21, no. 19, pp. 21159-21174, 2021. [CrossRef] [Google Scholar] [Publisher Link]

[14] Kamal Kumar Gola, and Shikha Arya, "Underwater Acoustic Sensor Networks: Taxonomy on Applications, Architectures, Localization Methods, Deployment Techniques, Routing Techniques, and Threats: A Systematic Review," *Concurrency and Computation: Practice and Experience*, vol. 35, no. 23, 2023. [CrossRef] [Google Scholar] [Publisher Link]

[15] Brahim Benaissa et al., "Metaheuristic Optimization Algorithms: An Overview," *HCMCOU Journal of Science-Advances in Computational Structures*, vol. 14, no. 1, pp. 33-61, 2024. [CrossRef] [Google Scholar] [Publisher Link]

[16] A. Hanif Halim, Idris Ismail, and Swagatam Das, "Performance Assessment of the Metaheuristic Optimization Algorithms: An Exhaustive Review," *Artificial Intelligence Review*, vol. 54, no. 3, pp. 2323-2409, 2021. [CrossRef] [Google Scholar] [Publisher Link]

[17] Laith Abualigah et al., "Meta-Heuristic Optimization Algorithms for Solving Real-World Mechanical Engineering Design Problems: A Comprehensive Survey, Applications, Comparative Analysis, and Results," *Neural Computing and Applications*, vol. 34, no. 6, pp. 4081-4110, 2022. [CrossRef] [Google Scholar] [Publisher Link]

[18] Sibo Sun et al., "High-Precision Underwater Acoustic Localization of the Black Box Utilizing an Autonomous Underwater Vehicle Based on the Improved Artificial Potential Field," *IEEE Transactions on Geoscience and Remote Sensing*, vol. 61, pp. 1-10, 2023. [CrossRef] [Google Scholar] [Publisher Link]

[19] Sanyam Jain, "DeepSeaNet: Improving Underwater Object Detection Using EfficientDet," *2024 4th International Conference on Applied Artificial Intelligence (ICAPAI)*, Halden, Norway, pp. 1-11, 2024. [CrossRef] [Google Scholar] [Publisher Link]

[20] Sibo Sun et al., "High-Precision Underwater Acoustical Localization of the Black Box Based on an Improved TDOA Algorithm," *IEEE Geoscience and Remote Sensing Letters*, vol. 18, no. 8, pp. 1317-1321, 2021. [CrossRef] [Google Scholar] [Publisher Link]

[21] Sibo Sun et al., "Underwater Acoustical Localization of the Black Box Utilizing Single Autonomous Underwater Vehicle Based on the Second-Order Time Difference of Arrival," *IEEE Journal of Oceanic Engineering*, vol. 45, no. 4, pp. 1268-1279, 2020. [CrossRef] [Google Scholar] [Publisher Link]

[22] Sibo Sun et al., "Underwater Acoustic Localization of the Black Box Based on Generalized Second-Order Time Difference of Arrival (GSTDOA)," *IEEE Transactions on Geoscience and Remote Sensing*, vol. 59, no. 9, pp. 7245-7255, 2021. [CrossRef] [Google Scholar] [Publisher Link]

[23] Michael A. Ainslie, and James G. McColm, "A Simplified Formula for Viscous and Chemical Absorption in Sea Water," *The Journal of the Acoustical Society of America*, vol. 103, no. 3, pp. 1671-1672, 1998. [CrossRef] [Google Scholar] [Publisher Link]

[24] Mari Carmen Domingo, "Overview of Channel Models for Underwater Wireless Communication Networks," *Physical Communication*, vol. 1, no. 3, pp. 163-182, 2008. [CrossRef] [Google Scholar] [Publisher Link]